Development/Plasticity/Repair

Astrocytes Are the Source of TNF Mediating Homeostatic Synaptic Plasticity

Renu Heir,* Zahra Abbasi,* Pragya Komal, Haider F. Altimimi, Marie Franquin, ⬤Dionysia Moschou, ⬤Julien Chambon, and David Stellwagen

Department of Neurology and Neurosurgery, Centre for Research in Neuroscience, Research Institute of the McGill University Health Center, Montréal, Quebec H3G 1A4, Canada

Tumor necrosis factor α (TNF) mediates homeostatic synaptic plasticity (HSP) in response to chronic activity blockade, and prior work has established that it is released from glia. Here we demonstrate that astrocytes are the necessary source of TNF during HSP. Hippocampal cultures from rats of both sexes depleted of microglia still will increase TNF levels following activity deprivation and still express TTX-driven HSP. Slice cultures from mice of either sex with a conditional deletion of TNF from microglia also express HSP, but critically, slice cultures with a conditional deletion of TNF from astrocytes do not. In astrocytes, glutamate signaling is sufficient to reduce NFκB signaling and TNF mRNA levels. Further, chronic TTX treatment increases TNF in an NFκB-dependent manner, although NFκB signaling is dispensable for the neuronal response to TTX-driven HSP. Thus, astrocytes can sense neuronal activity through glutamate spillover and increase TNF production when activity falls, to drive HSP through the production of TNF.

Key words: astrocyte; cytokine; homeostatic plasticity; mGluR; microglia; TNF

Significance Statement

The inflammatory cytokine tumor necrosis factor α (TNF) can mediate homeostatic synaptic plasticity (HSP), an adaptive form of circuit level synaptic plasticity, but the source of TNF had not been identified. Here we demonstrate that astrocytes are the critical source of TNF during homeostatic plasticity and define a pathway by which the astrocytes could monitor the local neuronal activity levels. This provides key information on how the astrocyte–neuron circuit functions to maintain neuronal activity within a normal range. This has important mechanistic information about the adaptive changes that occur during development and in response to disruptions of normal neuronal circuit function.

Introduction

Homeostatic synaptic plasticity (HSP) is an important form of plasticity that provides stability to neuronal circuits (Turrigiano, 2007; Chen et al., 2022). It is a type of negative feedback where increased levels of neuronal firing over long-time scales result in the weakening of excitatory synapses, while chronic activity blockade results in stronger excitatory synapses.

At least one major type of HSP is mediated by the pro-inflammatory cytokine tumor necrosis factor α (TNF) in

response to activity deprivation (Stellwagen and Malenka, 2006; Heir and Stellwagen, 2020). TNF is secreted from glia after extended activity deprivation and triggers the trafficking of AMPARs to the neuronal surface in order to strengthen synapses. A requirement for involvement in synaptic scaling, then, is the ability to express and secrete TNF in response to changes in activity levels. While previous work conclusively establishes glia as the source of TNF in synaptic scaling, it is unclear which subtype of glia contributes and under what conditions. There are four main subtypes of glia in the CNS—microglia, astrocytes, oligodendrocytes, and NG2 cells. Of these, there are no current reports of TNF expression in either oligodendrocytes or NG2 cells, so we focused instead on microglia and astrocytes as candidates.

Microglia produce TNF in culture (Sawada et al., 1989), and microglial TNF secretion has been studied extensively in the context of neuroinflammation and neurodegenerative disease (Hanisch, 2002; Smith et al., 2012). Microglia are capable of producing large quantities of TNF and therefore are an intriguing possibility in terms of the source of TNF during synaptic scaling.

However, astrocytes also produce TNF in culture (Sawada et al., 1989), and astrocytic TNF secretion has been observed in the CNS response to inflammatory insults (Chung and Benveniste, 1990; Dong and Benveniste, 2001). That, combined with their close association with synapses (Perea et al., 2009), makes them an attractive candidate for the source of TNF during synaptic scaling as well.

Indeed, both types of glia have been shown to contribute to TNF-mediated changes in neural circuits and behavior—astrocytes for the response to antidepressants (Duseja et al., 2014) and microglia for the response to stress or cocaine (Lewitus et al., 2016; Kemp et al., 2022). Thus, it is an active question of how TNF is regulated during HSP. The type of glia involved will also have implications for how glia could monitor neuronal activity.

There is a great deal of uncertainty about how glia sense neuronal activity during HSP. Neurons release a number of signals that are proportional to neuronal firing rates or overall circuit activity. Perhaps the simplest option would be the overall level of extracellular glutamate, which would reflect the firing rates of local excitatory neurons. As higher extracellular glutamate would correlate with higher levels of circuit activity, this would suggest that glutamate signaling would suppress glial TNF levels (which rise when circuit activity and thus extracellular glutamate drop for sustained periods). And indeed, prior work has shown that glial TNF levels decrease following glutamate treatment (Stellwagen and Malenka, 2006). The mechanistic nature of this suppression, however, has not been determined. Although TNF transcription is regulated via NFκB signaling, a number of other control pathways also exist (Hayden et al., 2006).

Here, we determine that microglia are unnecessary for homeostatic plasticity and that the TNF-secreting glial subtype required for TNF during HSP is the astrocyte. Furthermore, astrocyte TNF is regulated by mGluRs via modulating NFκB signaling.

Materials and Methods

Animals. Floxed TNF mice were obtained from S. Nedospasov (Kuprash et al., 2005) and crossed with GFAP-Cre mice (Bajenaru et al., 2002) from NCI Mouse Repository or with Tg(CX3CR1-Cre) MW126Gsat mice (Yona et al., 2013) generated by N. Heintz (The Rockefeller University, GENSAT) and purchased from MMRRC (UC Davis). GFAP or CX3CR1-Cre-expressing mice were compared with GFAP or CX3CR1-Cre-nonexpressing littermates. Floxed TNF and GFAP-Cre mice were on a C57/Bl6 background; Cx3Cr1-Cre mice were a mix of FVB/B6/129/Swiss/CD1. Wild-type Sprague Dawley rats were obtained from Charles River Laboratories. All animal procedures were performed in accordance with the guidelines of the Canadian Council on Animal Care and the Montreal General Hospital Facility Animal Care Committee.

Cortical neuron–glial cultures. Cortical neuron–glial cultures were generated using established protocols outlined in Beattie et al. (2002). Briefly, E17/18 embryos of either sex were removed from pregnant Sprague Dawley rat females (Charles River Laboratories), and cortices were dissected from the brains. 0.05% trypsin-EDTA (Thermo Fisher) followed by physical trituration with a fire-polished Pasteur pipet was used to dissociate the tissue into a cell suspension. Cells were plated onto nitric acid-treated and poly-D-lysine (Sigma)-coated coverslips (Thermo Fisher) for imaging, or onto poly-D-lysine-coated cell culture dishes (Sarstedt) for mRNA experiments. Cultures were grown in Neurobasal supplemented with B27 and 0.25% GlutaMAX (Thermo Fisher). Glial growth was inhibited using 5-fluoro-2′-deoxyuridine (FUDR) at 14–18 DIV if necessary. Cells were used for experiments at 21–23 DIV. Experiments were done on a minimum of three separate culture preparations.

Glial cultures. Mixed glial cultures were generated from P0 Sprague Dawley rat pups of either sex. Briefly, cortices were dissected and dissociated using 0.05% trypsin-EDTA and physical trituration with a fire-polished Pasteur pipet. Cells were plated into cell culture flasks (Sarstedt) and grown to confluence in MEM supplemented with 5% FBS, 1% GlutaMAX, and 3.825 g/L D-glucose. Neurons were removed by gently hitting the flask to mechanically dislodge them before passaging. Astrocyte-only cultures were generated by taking confluent mixed glial cultures and treated them for 5–6 d with 8 μM cytosine arabinoside (AraC; Sigma) followed by a 45 min treatment with 75 mM L-leucine methyl ester (LME; Sigma). Cells were then passaged into cell culture dishes the next day and then used for experiments 2–3 d after that.

Organotypic hippocampal slice cultures. TNF^flox/flox animals were crossed with TNF^flox/flox; GFAP^− or CX3CR1-Cre^+/− in order to generate both TNF flox/flox; Cre^+/− and TNF flox/flox; Cre^−/− animals that would serve as wild-type littermate controls. Hippocampal slice cultures were made from P6 to P7 mouse pups of either sex. Briefly, hippocampi were dissected from pups and then sliced using a McIlwain tissue chopper in order to generate 300 μM slices. Slices were then cultured on PTFE cell culture inserts (Millipore) in media containing 50% MEM with HEPES and GlutaMAX, 25% horse serum sourced from New Zealand, 25% Hank's balanced salt solution (HBSS), and 6.5 g/L D-glucose. Slice cultures were harvested for mRNA or used for mEPSC recordings at 7–8 DIV.

Drug treatments. L-Glutamic acid (Tocris) and N-methyl-D-aspartate (NMDA; Tocris) were solubilized in water and applied to astrocyte cultures at a concentration of 100 μM. (RS)-3,5-DHPG (Tocris) was solubilized in water and used at 20 μM. Bay 11-7085 was dissolved in DMSO and used at 40 μM with the appropriate vehicle control for 16 h, with treatment with 1 μM TTX (Hello Bio) for 24 h.

Transfections. Coverslips to be transfected with any one construct were moved to a 3.5 cm dish with 1 ml pre-conditioned medium. A 0.1 ml total calcium phosphate precipitate solution was added by mixing 0.05 ml solution of 250 mM $CaCl_2$ containing 5 μg plasmid DNA, to 0.05 ml solution of the following (in mm): 140 NaCl, 1.5 Na_2HPO_4, and 50 HEPES, pH adjusted to 7.05. Cells were incubated with the calcium precipitate solution for ~3 h, after which the phosphate precipitate was dissolved by 1:30 dilution of solution with 300 mM MES, pH adjusted to 5.5, added for ~30 s, after which coverslips are returned to their original well. Transfections were conducted at DIV 18–20, with 1 μM TTX being applied for 48 h starting the next day (DIV 19–21) before patch-clamp recordings. Only GFP-positive neurons were used for recordings. Constructs were obtained from Dr. Philip A. Barker and are described in Methot et al. (2013).

qPCR. mRNA was collected from cells using the RNeasy mini extraction kit (Qiagen) and was reverse transcribed into cDNA using 500 ng input mRNA using the QuantiTect reverse transcription kit (Qiagen). qRT-PCR was carried out using the Fast SYBR green master mix (Applied Biosystems). All assays were performed using the StepOne Plus instrument (Applied Biosystems). Primer sequences, annealing temperatures, and concentrations for SYBR green assays were as follows:

rat TNF: 60.5°C annealing, 600 nM
    fwd: CTT CTG TCT ACT GAA CTT CGG G
    rev: CTA CGG GCT TGT CAC TCG

rat GAPDH: 61.5°C annealing, 350 nM
    fwd: TTG TGG ATC TGA CAT GCC G
    rev: TGG GAG TTG CTG TTG AAG TC

All quantification was performed using the $\Delta\Delta C_t$ method using GAPDH as a reference gene after verifying that the amplification

efficiency was between 95 and 105%. Statistical analysis was performed by comparing $-\Delta\Delta C_t$ values.

Western blotting. Glial lysates were prepared in RIPA buffer (20 mM Tris, 1 mM EDTA, 140 mM NaCl, 1% Triton X-100, 0.1% SDS, 0.1% deoxycholate) supplemented with protease inhibitor cocktail (BioShop). Protein concentration was determined using the BCA assay kit (Pierce), and equal quantities of protein were loaded on a 10% polyacrylamide gel. Gels were transferred onto supported nitrocellulose membrane (Biorad) and probed with: anti-α-tubulin (Millipore) and anti-IκBα (Cell Signaling). Western blots were exposed onto autoradiography film (Denville Scientific) and band intensities quantified using ImageJ software (NIH).

Immunocytochemistry. For AMPAR surface labeling, cell cultures were fixed on ice in 2% paraformaldehyde in aCSF, followed by incubation with blocking buffer (2% normal goat serum, 3% bovine serum albumin in PBS) at room temperature. Nonpermeabilized cells were treated with N-terminal anti-GluA1 antibodies (NeuroMab; 1:200). Cells were then washed with PBS and then incubated with secondary Alexa Fluor antibodies (1:1,000; Thermo Fisher), followed by washing with PBS. Coverslips were mounted in Fluoromount G (Thermo Fisher) for imaging. For all nonsurface staining, cells were blocked in buffer also containing 0.1% Triton X-100.

For TNF labeling, cultures were treated for 4 h with a protein transport inhibitor cocktail (eBioscience, catalog #00-4980-93) to prevent the cleavage and release of TNF protein. Coverslips were then fixed (4% paraformaldehyde; 20 min), washed with 0.05% Tween in PBS, and incubated in blocking buffer (2% NGS, 2% BSA, 0.1% triton in PBS). Primary anti-TNF antibody (1:100, Abcam, catalog #AB215188) was incubated overnight at 4°, followed by secondary antibodies (as above) and DAPI (to label cell nuclei).

Image acquisition and analysis. Images were acquired on an epifluorescence microscope (Olympus BX61) with a CCD camera (Hamamatsu Orca R-2) using a 63× objective. Analysis of surface receptors was carried out using ImageJ software (NIH) essentially as described previously (Stellwagen et al., 2005). Briefly, images were obtained using identical acquisition conditions, with nontreated and treated cells from the same culture preparation always compared with each other. The total thresholded area of fluorescently labeled, surface AMPARs was measured automatically by the ImageJ software and divided by the total cell area, which was determined by setting a lower threshold level to measure background fluorescence produced by the fixed cells. For each experiment, the fluorescence of all cells was normalized by dividing by the average fluorescence of the untreated control cells. For TNF labeling, images were acquired at 20× on an Olympus FV1000 confocal microscope using identical settings for all images. Images were analyzed using ImageJ with areas of TNF labeling identified using the Otsu algorithm to define ROIs, and the mean fluorescence intensity (MFI) measured for those ROIs. The integrated density was calculated from the MFI multiplied by the total area of ROIs and normalized for cell number in the field of view (by number of DAPI-labeled nuclei).

Electrophysiology. For slice cultures, mEPSCs were recorded from CA1 pyramidal neurons using the whole-cell patch-clamp method in external solution (aCSF) containing (in mM) the following: 119 NaCl, 26.3 NaHCO₃, 2.5 KCl, 1.0 NaH₂PO₄, 11 glucose, 2.5 CaCl₂, 1.3 MgCl₂ and supplemented with 1 µm TTX and 50 µm picrotoxin. For dissociated cultures, aCSF contained (in mm) the following: NaCl 135, KCl 3.5, CaCl₂ 2, MgCl₂ 1.3, HEPES 10, D-glucose 20, pH adjusted to 7.3–7.4 with NaOH), supplemented with TTX (0.5 µm), picrotoxin (100 µm), and D-APV (25 µm). Recording pipets were pulled from borosilicate glass (King Precision Glass) so that they had a resistance of 3–6 MΩ and were filled with an internal solution composed of (in mM) the following: 122 Cs-gluconate, 8 NaCl, 10 glucose, 1 CaCl₂, 10 HEPES, 10 EGTA, 0.3 Na₃-GTP, and 2 Mg-ATP. Cells with stable access resistance <40 MΩ were deemed acceptable for analysis, which was carried out using the template search method (pCLAMP) and a threshold of 6 pA (slice culture) or 7 pA (dissociated culture). For slice culture, cells with

mEPSC frequency >4 Hz were excluded from analysis. For dissociated culture, cells with membrane resistance <150 MΩ, or very low mEPSC frequency (<0.2 Hz), were excluded from further analysis.

Statistics. All results are presented as the mean and SEM. Outliers were identified and excluded using Tukey outlier box plots. Parametric data were analyzed using two-way ANOVA, followed by post hoc *t* tests. Western blot, TNF fluorescence, and qPCR data were nonparametric and analyzed using either Wilcoxon tests or Mann–Whitney tests. Statistical analyses of qPCR data are performed on the $-\Delta\Delta C_t$ values rather than fold change because $\Delta\Delta C_t$ is a linear output of the assay. Calculation of fold change requires the use of exponents, making statistical analysis of these values more complex. However, fold change values are indicated on graphs as well, as they are more intuitive to understand. Due to having both up- and down-regulation in Figure 5B, only fold change was presented, though $-\Delta\Delta C_t$ values are given in the text and used for statistics.

Results

Generation of microglia-free astrocyte cultures

In order to study the role of glial subtypes in synaptic scaling, it is necessary to be able to generate cultures of single-cell types. Most of the methodology of astrocyte cultures is based on culture from rat brain tissue (McCarthy and de Vellis, 1980). A variation on this technique was used in order to generate Banker cultures used in the experiments characterizing the role of glia in synaptic scaling (Stellwagen and Malenka, 2006). While the method yields a culture that is predominantly astrocytic, contamination by other cell types including microglia was possible. Therefore, we used alternate techniques to isolate cell types in order to study the role of glia in more detail.

Microglia are the main contaminants of this type of cell culture: in cultures stained with antibodies for the astrocytic marker, the glial fibrillary acidic protein (GFAP), and the microglial marker ionized calcium-binding adapter molecule-1 (Iba-1), microglia are clearly present (Fig. 1A). Therefore, we utilized a method where contaminating microglia can be removed (Uliasz et al., 2012), which would allow for more definitive conclusions about the roles of individual cell types in biological processes. This protocol entails the treatment of confluent monolayers of glia with the antimitotic agent cytosine β-D-arabinofuranoside (AraC) for 4–6 d in order to deplete the still-proliferative microglia, while astrocytes have ceased dividing due to contact inhibition. This is followed by a brief treatment with L-leucine methyl ester (LME), a lysomotrophic agent which
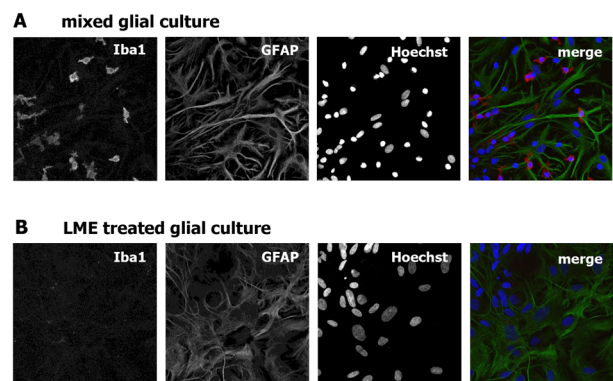
Figure 1. Microglia can be efficiently removed from cultures. *A*, Representative images of glial cultures stained with antibodies to an astrocyte marker (GFAP), microglial marker (Iba-1), nuclear stain (DAPI), and merged image showing microglia are clearly present in glial cultures. *B*, Representative micrographs of glial cultures depleted of microglia with AraC and LME treatment, using the same markers.

was originally used as a macrophage toxin (Thiele et al., 1983) and is used here for its toxicity to the closely related microglia. Staining of these cultures for astrocytic and microglial markers revealed an effective depletion of microglia (Fig. 1B), leaving behind a very enriched culture of astrocytes.
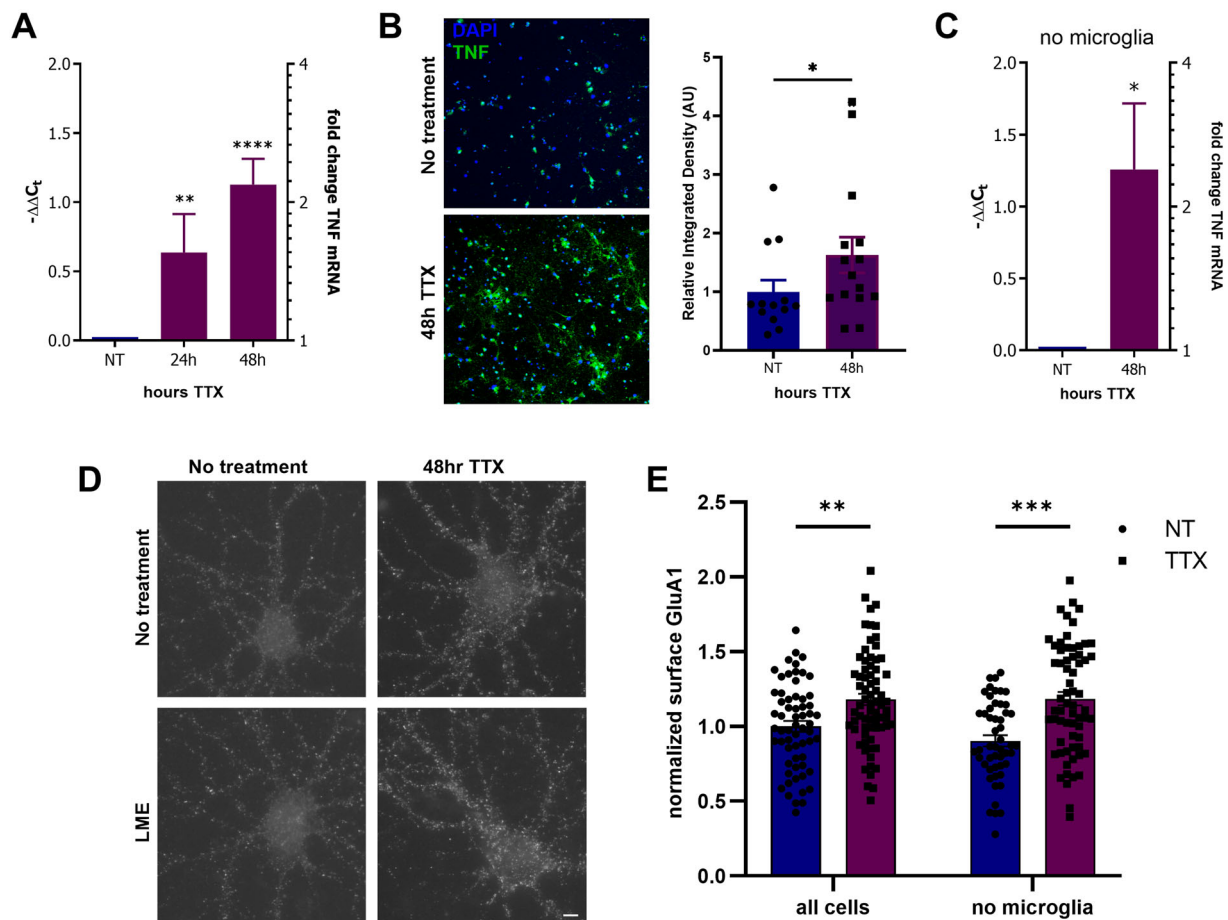
Microglia are dispensable for homeostatic synaptic plasticity in dissociated neuron-glial culture

The TNF-mediated modulation of neurotransmitter receptors during synaptic scaling is a relatively slow process, with changes taking at least 24 h to manifest (Stellwagen and Malenka, 2006). Much of the regulation of TNF occurs at the mRNA level (Carballo et al., 1998; Kontoyiannis et al., 1999; Falvo et al., 2010), so we quantify mRNA levels in neuron–glial cultures using reverse-transcription quantitative polymerase chain reactions (RT-qPCRs).

We conducted a time course experiment in rat cortical neuron–glial cultures, looking at TNF mRNA levels during prolonged TTX treatment. There is a significant increase in TNF

mRNA at 24 h treatment (Fig. 2A: $-\Delta\Delta C_t$ 24 h = 0.6353 ± 0.2793, Wilcoxon test $p < 0.01$, $n = 10$) and at 48 h (Fig. 2A: $-\Delta\Delta C_t$ 48 h = 1.1268 ± 0.1865, Wilcoxon test $p < 0.0001$, $n = 10$), in line with previous studies. Furthermore, the values obtained were well within the detection limit of the assay. Although we have previously observed good alignment between TNF mRNA and protein levels (Lewitus et al., 2016), we verified that the increase in TNF mRNA was accompanied by an increase in TNF protein. We treated cultures with TTX for 48 h and inhibited protein transport for the last 4 h to trap TNF protein within cells. We then immunostained for TNF and observed a significant increase in TNF fluorescent signal (Fig. 2B: TTX = 1.628 ± 0.303; Mann–Whitney $p = 0.041$, $n = 13–15$).

In order to test whether the presence of microglia is required for the TTX-induced increase in TNF mRNA, neuron–glial cultures were treated with mitotic inhibitors and subsequently treated with LME to deplete microglia. Depleted cultures did not stain positively for microglial markers (Fig. 1B). Despite the depletion, treatment with TTX for 48 h still resulted in an

Figure 2. Microglia are dispensable for synaptic scaling in dissociated neuron–glial culture. **A**, Dissociated cortical neuron–glial cultures were treated with 1 μM TTX and then assessed for TNF mRNA levels by qRT-PCR. $-\Delta\Delta C_t$ values are plotted on the left axis, while fold change is plotted on the right axis on a logarithmic scale. TNF mRNA was significantly elevated from nontreated cultures at 24 h ($-\Delta\Delta C_t$ 24 h = 0.6353 ± 0.279; Wilcoxon test $p < 0.01$, $n = 10$) and at 48 h ($-\Delta\Delta C_t$ 48 h = 1.127 ± 0.187; Wilcoxon test $p < 0.0001$, $n = 10$). **B**, TNF protein was also elevated by 48 h TTX treatment. Micrographs of neuron–glial cultures immunostained for TNF (green) and DAPI (blue) of nontreated and 48 h TTX treated cultures. The relative integrated density of fluorescence of TNF was increased by TTX treatment (NT = 1 ± 0.201, TTX = 1.628 ± 0.303; Mann–Whitney $p = 0.041$, $n = 13–15$). **C**, Dissociated cortical neuron–glial cultures were depleted of microglia, treated with 1 μM TTX for 48 h, and then assessed for TNF mRNA levels to reveal strong trend toward increased TNF mRNA as compared to non-TTX-treated cultures ($-\Delta\Delta C_t$ TTX = −0.852 ± 0.297; Mann–Whitney $p = 0.1188$, $n = 5$). **D**, Representative images of nonpermeabilized neuron–glial cultures stained for GluA1. Scale bar = 1 μm. Control cultures and microglia-depleted cultures were treated with TTX for 48 h and then assessed for surface GluA1 staining. **E**, Quantification of data from (**D**), with all data normalized to nontreated control cultures. A two-way ANOVA examining the effect of TTX × LME treatment was performed. A significant main effect of TTX on surface GluA1 was found ($F_{(1,245)} = 33.13$, $p < 0.0001$). The TTX × LME treatment interaction was not significant ($F_{(1,245)} = 1.595$, $p = 0.2077$). Post hoc t tests show that TTX increases surface GluA1 in non-LME-treated cultures (NT = 1.00 ± 0.036, TTX = 1.181 ± 0.038, $p = 0.0011$, $n = 133$) as well as in LME-treated cultures (LME = 0.9028 ± 0.0379, LME + TTX = 1.184 ± 0.045, $p < 0.0001$, $n = 116$).

increase in TNF mRNA (Fig. 2C: $-\Delta\Delta C_t$ TTX $= -1.258 \pm 0.460$, Mann–Whitney $p = 0.0152$, $n = 7$), indicating that microglia were dispensable for this process. These data suggest that astrocytes, therefore, are the likely source of TNF during synaptic scaling.

We then verified that microglia were also unnecessary for the neuronal changes during up-scaling, which are downstream of TNF production. Activity deprivation of neuron–glial cultures with TTX for 48 h increases surface GluA1 immunostaining (Stellwagen and Malenka, 2006), so we use this as a measure of surface AMPARs. To confirm this finding in our cultures, we performed nonpermeabilized staining of neuron–glial cultures either with or without microglial depletion with antibodies to GluA1 after 48 h TTX (Fig. 2D,E). A two-way ANOVA revealed a significant main effect of TTX on surface GluA1 ($F_{(1,245)} = 33.13$, $p < 0.0001$), but the TTX × LME treatment interaction was not significant ($F_{(1,245)} = 1.595$, $p = 0.2077$). Post hoc tests show that TTX increases surface GluA1 in non-LME-treated cultures (NT $= 1.000 \pm 0.036$, TTX $= 1.181 \pm 0.038$, $p = 0.0011$, $n = 133$) as well as in LME-treated cultures (LME $= 0.9028 \pm 0.0379$, LME + TTX $= 1.184 \pm 0.045$, $p < 0.0001$, $n = 116$). Therefore, depletion of microglia from cultures did not prevent the activity deprivation-induced increase in TNF or increase in surface AMPARs, indicating that microglia are not required for synaptic up-scaling in dissociated cultures.

Astrocytic TNF is required for synaptic scaling in organotypic hippocampal slice cultures
While dissociated neuron–glial cultures are a useful system that has been used extensively for homeostatic plasticity studies, they are not ideal for testing the contribution of microglia. First, glial proliferation is routinely inhibited (Brewer et al., 1993), which keeps glia from over-running the postmitotic neurons, but also means that these cultures may not be ideal for studying glial effects on neurons. More importantly, there are few to no observable microglia to begin with in dissociated neuron–glial cultures (unlike mixed glial cultures used in Fig. 1; Iba-1 staining, data not shown), which could be a confounding factor in interpreting the relative contributions of glial subtypes to synaptic scaling. Therefore, we sought to examine the roles of glial subtypes in a more physiologically intact system, with all glial subtypes represented.

To this end, we examined synaptic scaling in organotypic hippocampal slice cultures. In this preparation, slices of neonatal hippocampal tissue are grown on a porous membrane with organotypic organization preserved (Stoppini et al., 1991). These cultures express robust synaptic scaling (Stellwagen and Malenka, 2006), so it could be an appropriate system to look at glial subtype contribution. Importantly, microglia have been studied extensively in organotypic hippocampal slice cultures and are present in large enough numbers for analysis (Hailer et al., 1996; Dailey and Waite, 1999; Stence et al., 2001), so using this system allows the study of the contributions of both astrocytes and microglia to synaptic scaling.

In order to confirm that slice cultures behave similarly to dissociated cultures, we first assayed TNF mRNA in rat hippocampal slice cultures after 48 h TTX treatment. As expected, a robust increase in TNF mRNA was observed (Fig. 3A: $-\Delta\Delta C_t$ TTX $= 0.8880 \pm 0.2118$, Mann–Whitney $p < 0.001$, $n = 5$ for both conditions).

Depletion of microglia with the same protocol used in dissociated culture was not possible, as the time needed for LME to penetrate the tissue was long enough that the viability of other cell types was affected (data not shown). Therefore, an alternate method to assess the contribution of microglia to TNF-mediated synaptic scaling was necessary. To address this problem, we used the Cre-loxP system in order to carry out a cell-type-specific knock-out of TNF. Floxed TNF mice (Kuprash et al., 2005) were crossed with C-X3-C motif chemokine receptor 1 (CX3CR1)-Cre mice (Yona et al., 2013) in order to generate microglial TNF knock-outs. In the brain, this Cre line is specific to microglia, though it does affect a small population of neurons (Lewitus et al., 2016) as well as macrophages peripherally. Given that neuronal TNF is not required for synaptic scaling (Stellwagen and Malenka, 2006), its loss in a subset of nonhippocampal neurons is unlikely to affect the analysis.

Immunocytochemistry for surface receptors as performed in dissociated cultures is not feasible in organotypic hippocampal slice cultures, as the staining would be too dense to quantify. For that reason, we performed patch-clamp recordings of mEPSCs in CA1 neurons to assess synaptic strength after activity deprivation in CX3CR1-Cre− and CX3CR1-Cre+ cultures. Deletion of TNF from microglia did not prevent the homeostatic increase in mEPSC amplitude in CA1 neurons following TTX treatment (Fig. 3B,C). A two-way ANOVA showed a significant main effect of TTX on mEPSC amplitude ($F_{(1,46)} = 7.997$, $p = 0.0069$) as well as a significant main effect of genotype on mEPSC amplitude ($F_{(1,46)} = 50.782$, $p < 0.0001$). However, the genotype × TTX interaction was not significant ($F_{(1,46)} = 0.095$, $p = 0.759$), suggesting that both wild-type and microglial TNF knock-out slice cultures respond similarly to activity deprivation. This was confirmed with post hoc tests showing that in wild-type cultures, mEPSC amplitude is significantly increased with TTX (CX3CR1-Cre−: NT $= 18.02 \pm 1.13$ pA, TTX $= 20.41 \pm 0.96$ pA, $p = 0.045$) and in cultures lacking microglial TNF (CX3CR1-Cre+: NT $= 11.06 \pm 0.73$ pA, TTX $= 14.19 \pm 0.75$ pA, $p = 0.028$). This demonstrates that microglial TNF is not required for synaptic scaling.

It is interesting to note that baseline mEPSC amplitude differed between the two genotypes. Slice cultures lacking microglial TNF had significantly lower mEPSC amplitude ($p < 0.0001$), suggesting that TNF from microglia is required to set or maintain baseline synaptic strength or that the loss of TNF results in the release of other microglial factors that impact synaptic function.

The above data would imply that if the TNF supplied by glia during synaptic scaling is not coming from microglia, it is most likely secreted by the other major glial type present, astrocytes. In order to address this question more directly, we made use of the GFAP-Cre line that is astrocyte-specific, though it does express Cre in a small population of neurons (Lewitus et al., 2016). We performed mEPSC recordings in CA1 neurons following TTX treatment and revealed the loss of homeostatic compensation (Fig. 3D,E). A two-way ANOVA showed a significant main effect of TTX on mEPSC amplitude ($F_{(1,31)} = 4.7166$, $p = 0.0376$) and a significant main effect of genotype ($F_{(1,31)} = 4.5588$, $p = 0.0408$). Critically, the genotype × TTX interaction was significant ($F_{(1,31)} = 5.1163$, $p = 0.0309$), suggesting that response to activity deprivation depends on the genotype of the slice cultures. Post hoc tests indicate that in wild-type slice cultures, TTX significantly elevates mEPSC amplitude (GFAP-Cre −: NT $= 13.37 \pm 0.71$ pA, TTX $= 19.13 \pm 1.86$ pA, $p < 0.001$), but not in slice cultures lacking astrocytic TNF (GFAP-Cre+: NT $= 13.53 \pm 1.20$ pA, TTX $= 13.41 \pm 1.02$ pA, $p = 0.4744$). Therefore, astrocytic TNF is required for the increase in synaptic strength seen during synaptic scaling in response to activity deprivation.
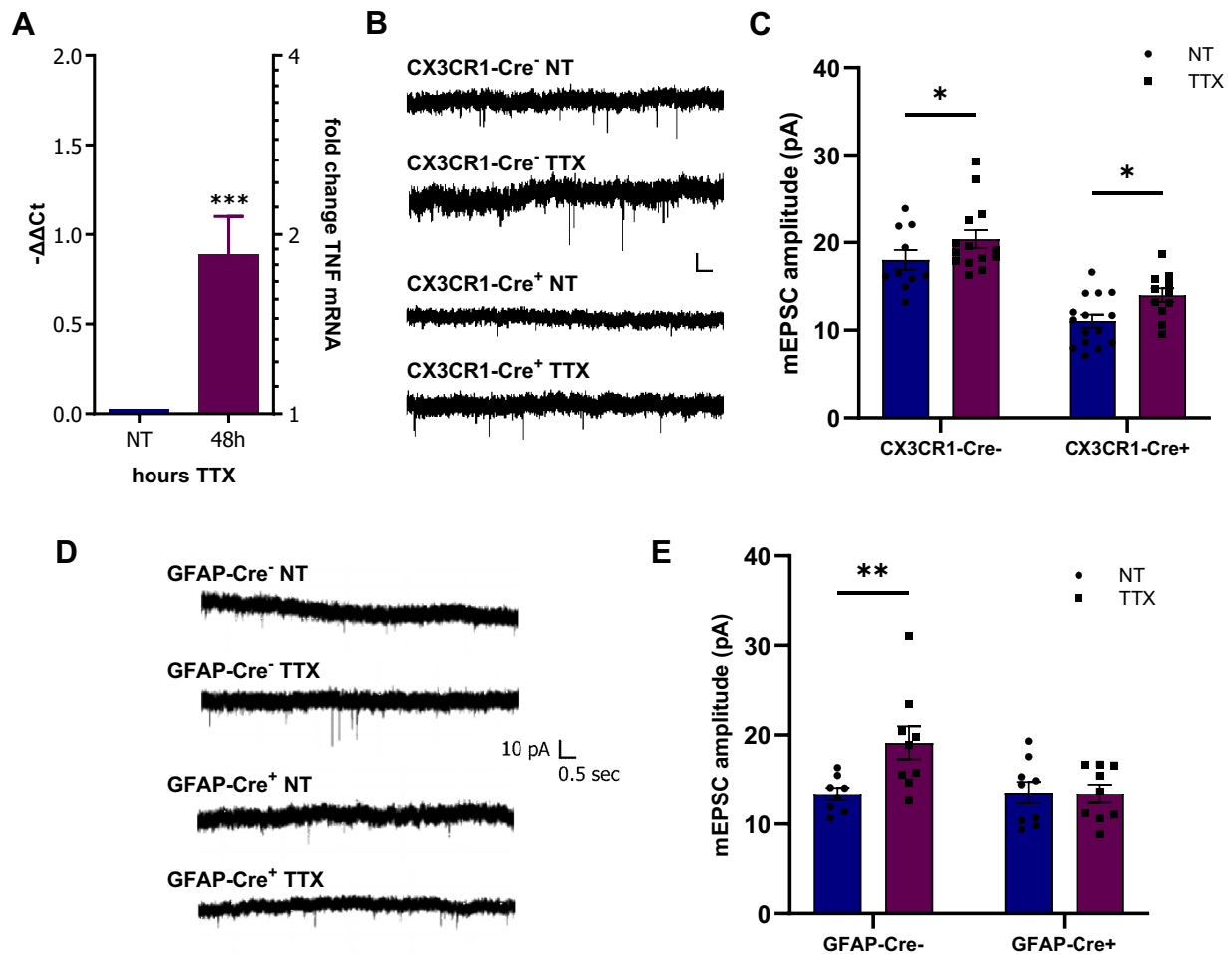
Figure 3. Astrocytic TNF is required for synaptic scaling in organotypic hippocampal slice cultures. **A**, Rat hippocampal slice cultures were treated with 1 μM TTX for 48 h and then assessed for TNF mRNA levels by qRT-PCR. Slice cultures treated with TTX had significantly higher TNF mRNA ($-\Delta\Delta C_t$ TTX = 0.888 ± 0.212, Mann–Whitney $p < 0.001$, $n = 5$ for both conditions). **B**, Representative traces of mEPSCs from the CA1 of hippocampal slice cultures from CX3CR1-Cre− and CX3CR1-Cre+ mice nontreated or treated with 48 h TTX. **C**, Quantification of mEPSC amplitude in (**B**). A two-way ANOVA examining the effect of genotype × TTX treatment demonstrated a significant main effect of TTX on mEPSC amplitude ($F_{(1,46)} = 7.9968$, $p = 0.0069$) and a significant main effect of genotype on mEPSC amplitude ($F_{(1,46)} = 50.7817$, $p < 0.0001$). However, the genotype × TTX interaction was not significant ($F_{(1,46)} = 0.0950$, $p = 0.7593$). Post hoc one-tailed t tests show that in wild-type cultures, mEPSC amplitude is significantly increased with TTX (CX3CR1-Cre−: NT = 18.01 ± 1.12 pA, TTX = 20.38 ± 1.03 pA, $p = 0.045$) and in cultures lacking microglial TNF (CX3CR1-Cre+: NT = 11.06 ± 0.73 pA, TTX = 13.99 ± 0.78 pA, $p = 0.028$). Additionally, baseline mEPSC amplitude is significantly decreased in cultures lacking microglial TNF (two-tailed t test, CX3CR1-Cre− NT vs CX3CR1-Cre+ NT, $p < 0.0001$). The dots represent recorded cells, from four to five different animals. **D**, Representative traces of mEPSCs from the CA1 of hippocampal slice cultures from GFAP-Cre− and GFAP-Cre+ animals nontreated or treated with 48 h TTX. **E**, Quantification of mEPSC amplitude in (**D**). A two-way ANOVA revealed a significant main effect of TTX on mEPSC amplitude ($F_{(1,31)} = 4.7166$, $p = 0.0376$) and a significant main effect of genotype on mEPSC amplitude ($F_{(1,31)} = 4.5588$, $p = 0.0408$). Importantly, the genotype × TTX interaction was significant ($F_{(1,31)} = 5.1163$, $p = 0.0309$). Post hoc one-tailed t tests indicate that in wild-type slice cultures, TTX significantly elevates mEPSC amplitude (GFAP-Cre−: NT = 13.37 ± 0.71 pA, TTX = 19.13 ± 1.86 pA, $p < 0.001$), but not in slice cultures lacking astrocytic TNF (GFAP-Cre+: NT = 13.53 ± 1.20 pA, TTX = 13.41 ± 1.02 pA, $p = 0.4744$). The dots represent recorded cells, from three to four different animals.
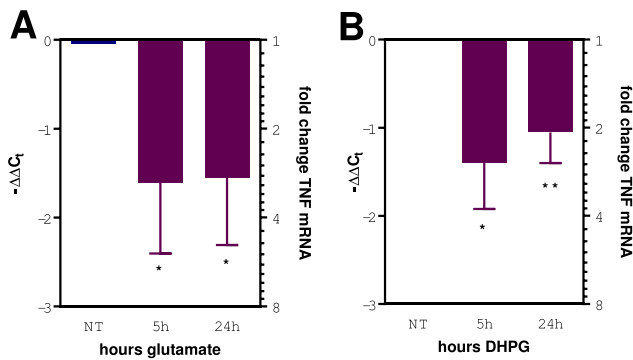
Glutamate reduces TNF mRNA levels through activation of group I mGluRs in astrocytes

We next examined how neurons may influence the production of TNF in astrocytes using astrocyte-only cultures. Previous work suggested that glutamate can reduce glial TNF production (Stellwagen and Malenka, 2006). Without neurons present, the astrocytes would not be detecting activity and should therefore maximally produce TNF in a homeostatic response. Treating astrocytes with glutamate, then, could approximate the presence of an active neural network and decrease TNF production. To confirm that glutamate modulates astrocyte TNF production, astrocytes were treated with a time course of 100 μM glutamate, and TNF mRNA levels were measured by RT-qPCR (Fig. 4A). TNF mRNA was significantly decreased after 5 h glutamate treatment ($-\Delta\Delta C_t$ 5 h = −1.607 ± 0.797; Wilcoxon test $p = 0.031$;

$n = 6$) and TNF remained depressed after 24 h glutamate treatment ($-\Delta\Delta C_t$ 24 h = −1.547 ± 0.7612; Wilcoxon test $p = 0.031$; $n = 7$).

To determine which glutamate receptor facilitates this signaling, we tested the involvement of mGluRs in the regulation of TNF. These receptors are found in several different subtypes: group I mGluRs are G_q G-protein-coupled receptors (GPCRs), whereas groups II and III mGluRs are $G_{i/o}$ GPCRs (Niswender and Conn, 2010). Group I mGluRs are an attractive candidate for involvement in synaptic scaling as the downstream effector of group I mGluRs is calcium, which is an important signaling mode for astrocytes, especially in the context of neuron–glial communication (Perea and Araque, 2005).

In order to test their involvement, astrocyte cultures were treated with 15 μM dihydroxyphenylglycine (DHPG), an agonist

Figure 4. Glutamate reduces TNF mRNA levels through activation of group I mGluRs. *A*, Astrocyte cultures were treated with 100 μM glutamate for the times indicated, followed by qRT-PCR for TNF mRNA levels. $-\Delta\Delta C_t$ values are plotted on the left axis, while fold change is plotted on the right axis on a logarithmic scale. TNF mRNA was significantly decreased after 5 h glutamate treatment ($-\Delta\Delta C_t$ 5 h = -1.61 ± 0.80; Wilcoxon test $p = 0.031$, $n = 6$) and remained depressed after 24 h glutamate treatment ($-\Delta\Delta C_t$ 24 h = -1.55 ± 0.76; Wilcoxon test $p = 0.031$, $n = 7$). *B*, Astrocyte cultures were treated with 15 μM DHPG for the times indicated, followed by qRT-PCR for TNF mRNA levels. TNF mRNA decreased significantly after 5 h treatment ($-\Delta\Delta C_t$ 5 h = -1.40 ± 0.52; Wilcoxon test $p = 0.02$, $n = 10$) and after 24 h treatment ($-\Delta\Delta C_t$ 24 h = -1.05 ± 0.35; Wilcoxon test $p = 0.007$, $n = 11$).

of group I mGluRs, and then assessed for TNF mRNA levels by RT-qPCR (Fig. 4B). Consistent with what we observed with glutamate treatment, TNF mRNA significantly decreased after 5 h treatment with DHPG ($-\Delta\Delta C_t$ 5 h = -1.40 ± 0.5208; Wilcoxon test $p = 0.0195$; $n = 10$) and was maintained at 24 h treatment ($-\Delta\Delta C_t$ 24 h = -1.054 ± 0.346; Wilcoxon test $p = 0.0068$; $n = 11$).

Astrocytes are also known to express NMDA receptors (Hogan-Cann and Anderson, 2016), which can also elevate intracellular calcium. We therefore also treated astrocyte cultures with 100 μM of NMDA for 4 h and 24 h. Unlike the decrease observed with DHPG, NMDA did not significantly alter TNF mRNA levels ($-\Delta\Delta C_t$ 4 h = 0.465 ± 0.631; $n = 4$; $-\Delta\Delta C_t$ 24 h = 0.720 ± 0.470; $n = 4$; Wilcoxon test $p = 0.63$ (4 h), 0.13 (24 h)), and the response trended in the opposite direction from the response to glutamate, making NMDARs unlikely to contribute to the observed glutamate response. Altogether, this suggests that glutamate, acting at least in part through metabotropic receptors, may be the activity signal to astrocytes during synaptic scaling.

TNF transcription is canonically controlled via NFκB signaling (Hayden et al., 2006). Additionally, it has been implicated in responses to glutamate in other cell types (Guerrini et al., 1995; Kaltschmidt et al., 1995) and even in responses to glutamate through group I mGluRs in particular (O'Riordan et al., 2006). Having established that glutamate can decrease TNF levels in astrocytes, we tested whether this is accompanied by changes in NFκB signaling, particularly in the level of the NFκB inhibitor IκBα (the nuclear factor of kappa light polypeptide gene enhancer in B-cell inhibitor, α). This protein binds and masks the nuclear localization signal (NLS) of NFκB, sequestering it in the cytoplasm where it cannot function as a transcription factor. Phosphorylation of IκBα by IκB kinase (IKK) signals its ubiquitination and subsequent proteasomal degradation, which reveals the NLS of NFκB, allowing it to translocate to the nucleus and function as a transcription factor.

Astrocyte cultures were treated with glutamate and assessed by Western blot for IκBα (Fig. 5A). In this case, because glutamate decreases TNF levels, we would expect IκBα to be increased, thus inhibiting the NFκB pathway and decreasing transcription

of TNF. Indeed, IκBα was significantly elevated after 24 h glutamate treatment (NT = 1.000 ± 0.150, 24 h = 3.339 ± 0.817; Wilcoxon test $p = 0.0313$; $n = 6$ for both conditions) as well as after 48 h glutamate treatment (48 h = 3.178 ± 0.605; Wilcoxon test $p = 0.0313$; $n = 6$), consistent with the idea that NFκB is negatively regulated by glutamate in astrocytes.

To test if NFκB signaling is regulating TNF levels during synaptic scaling, we treated dissociated neuron–glial cultures with the NFκB inhibitor Bay 11-7085 while blocking the activity with TTX. Vehicle-treated cultures upregulated TNF mRNA after 24 h TTX treatment, as expected (Fig. 5B; TTX: $-\Delta\Delta C_t$ = 1.816 ± 0.397; fold change = 4.19 ± 1.05; $p = 0.0313$; $n = 6$). Treatment of control cultures with Bay 11-7085 for 16 h did not significantly alter TNF levels (Bay11: $-\Delta\Delta C_t = -0.601 \pm 0.267$; fold change 0.691 ± 0.228; $p = 0.125$; $n = 4$), but critically 24 h TTX treatment did not elevate TNF mRNA when NFκB was inhibited for the last 16 h (Bay11 + TTX: $-\Delta\Delta C_t = -1.51 \pm 0.288$; fold change 0.488 ± 0.220; $p = 0.0625$ vs control, 0.213 vs Bay11; $n = 5$). This suggests that NFκB signaling in astrocytes is required for the increase in TNF seen in response to long-term activity blockade.

In addition to being upstream of TNF production, NFκB activation is also downstream of the TNF receptor. We therefore also wanted to test whether NFκB signaling in neurons is required for synaptic scaling. To this end, we utilized a construct transfected specifically into neurons to express a mutant form of IκBα, IκBαm, which cannot be phosphorylated, increasing its stability and allowing it to continue masking the NLS of NFκB, blocking the pathway (Methot et al., 2013). Sparse transfection of a control construct (GFP) or IκBαm (combined with GFP) was followed by 48 h TTX treatment and mEPSC recordings specifically from transfected neurons. TTX treatment strongly increased mEPSC amplitude, compared with untreated cultures, for both constructs (Fig. 5C,D). A two-way ANOVA showed a significant main effect of TTX on mEPSC amplitude ($F_{(1,91)} = 18.5276$, $p < 0.0001$) but no main effect of IκBαm expression ($F_{(1,91)} = 0.0217$, $p = 0.8833$) and no transfection × activity deprivation interaction ($F_{(1,91)} = 0.0004$, $p = 0.9851$). Post hoc tests revealed a significant increase in mEPSC amplitude after TTX treatment in neurons transfected with control construct (GFP: NT = 15.2379 ± 0.5389, TTX = 18.4784 ± 0.7636, $p < 0.001$), as well as in neurons transfected with NFκB inhibitor (IκBαm: NT = 15.3623 ± 0.6178, TTX = 18.5747 ± 1.0024, $p < 0.01$), indicating that synaptic scaling does not require neuronal NFκB signaling. This establishes a plausible NFκB-dependent pathway that controls TNF production in astrocytes to mediate HSP.

Discussion

Previously we had established that glial TNF mediates a form of HSP (Stellwagen and Malenka, 2006). Here we provide evidence that the glial source of TNF during homeostatic plasticity is in fact astrocytes. Following 2 d of activity blockade, TNF still increases in the absence of microglia to drive homeostatic plasticity. Deleting TNF from microglia also does not prevent HSP but critically deleting TNF from astrocytes does. Glutamate signaling down-regulates TNF production via inhibition of NFκB signaling, and blocking NFκB signaling prevents the upregulation of TNF driven by chronic activity blockade.

Overall, this positions astrocytes to be the primary sensor of neuronal activity during long-term TTX-driven HSP. Glia have shifted from being thought of as passive supporters of neuronal function to being active participants in many aspects of CNS
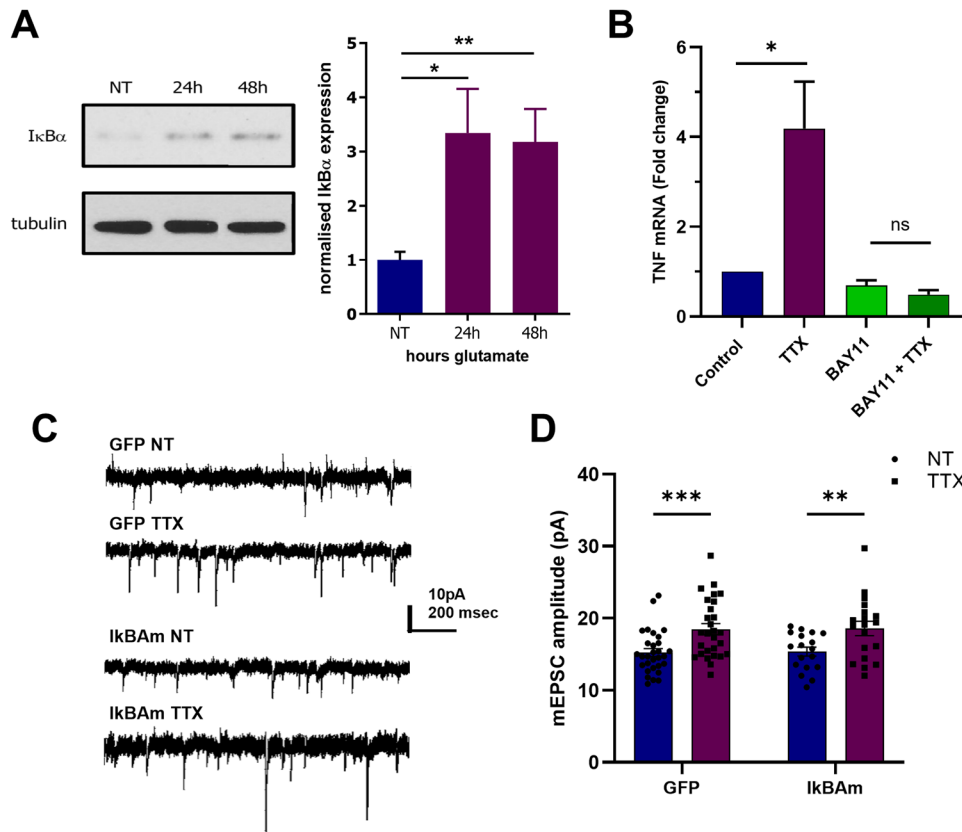
Figure 5. Non-neuronal NFκB is required for synaptic scaling. *A*, Glutamate treatment upregulates IκBα expression in astrocytes. Astrocyte cultures were treated with 100 μM glutamate for 24–48 h, and expression of IκBα and tubulin was measured by Western blot. Representative blots and group data demonstrate a strong upregulation of IκBα after glutamate treatment. Quantification of IκBα expression normalized to tubulin levels revealed that IκBα was significantly elevated after 24 h glutamate treatment (NT = 1.00 ± 0.15, 24 h = 3.34 ± 0.82; Wilcoxon test $p < 0.05$, $n = 6$ for both conditions) as well as after 48 h glutamate treatment (48 h = 3.18 ± 0.61; Wilcoxon test $p < 0.01$, $n = 6$). *B*, NFκB signaling is required for the TTX-mediated up-regulation of TNF. Mixed neuronal–glia cultures were treated with TTX for 24 h with or without the NFκB inhibitor, 40 μM Bay 11-7085 (TTX = 4.19 ± 1.05, $n = 6$; Bay11 = 0.71 ± 0.11, $n = 4$; Bay11 + TTX = 0.41 ± 0.10, $n = 5$; Wilcoxon test $p = 0.0313$, control vs TTX). *C*, Representative traces of mEPSCs obtained from dissociated hippocampal cultures treated with 1 μM TTX for 48 h with or without the sparse transfection of IkBαm to inhibit NFκB. *D*, Quantification of mEPSC data from (*C*). A two-way ANOVA of examining the effect of the NFκB inhibiting construct, IkBαm, and activity manipulation on mEPSC amplitude revealed a significant main effect of TTX on mEPSC amplitude ($F_{(1,91)} = 18.5276$, $p < 0.0001$), but there was no main effect of IkBαm on mEPSC amplitude ($F_{(1,91)} = 0.0217$, $p = 0.8833$) or a transfection × activity deprivation interaction ($F_{(1,91)} = 0.0004$, $p = 0.9851$). Post hoc tests revealed a significant increase in mEPSC amplitude after TTX treatment in cells transfected with control construct (GFP: NT = 15.24 ± 0.54, TTX = 18.48 ± 0.76, $p < 0.001$), as well as in cells transfected with the NFκB inhibitor (IkBαm: NT = 15.36 ± 0.62, TTX = 18.57 ± 1.00, $p < 0.01$), indicating that synaptic scaling does not require neuronal NFκB signaling. The dots represent recorded cells, from four different culture preparations.

function, including synaptic development (Ullian et al., 2001; Eroglu and Barres, 2010; Jones et al., 2011), elimination (Paolicelli et al., 2011; Chung and Barres, 2012), and plasticity (Ben Achour and Pascual, 2010). Astrocytes and microglia have both emerged as important players in regulating synaptic physiology. Both cell types are capable of responding to changes in activity levels at synapses. Microglia survey synapses by making direct contact with them (Wake et al., 2009) and can modify their motility behavior in response (Tremblay et al., 2010) as well as directly modify synapses (Schafer et al., 2012). Astrocytes are well known to respond to neuronal activity with calcium signaling (Cornell-Bell et al., 1990; Dani et al., 1992; Porter and McCarthy, 1996) and have already been implicated in several forms of plasticity (Yang et al., 2003; Perea and Araque, 2007; Gordon et al., 2009; Henneberger et al., 2010). Thus, both cell types are aptly positioned to participate in synaptic scaling.

Altogether, the data presented here implicate astrocytic TNF in the process of synaptic upscaling. In two different cell culture models, we show that microglial TNF is dispensable for synaptic scaling. Additionally, we show a requirement for astrocytic TNF in the more physiologically intact preparation of organotypic hippocampal slice cultures. These data are consistent with

previous reports using an entorhino-hippocampal slice culture system, where lesions of the inputs into the dentate gyrus were used as a model of HSP (Becker et al., 2013). The observed homeostatic response required TNF, with astrocytes expressing high levels of TNF in the denervated zone.

Astrocytic TNF is also required for the behavioral response to antidepressants, perhaps through the serotonin signaling to astrocytes (Duseja et al., 2014). However, microglia can clearly be a source of TNF as well, and microglial TNF is important to the response of other types of stimuli in vivo. In particular, microglial TNF is an important regulator of the synaptic and behavioral response to cocaine (Lewitus et al., 2016) and a driver of the synaptic plasticity and anxiety-like behavior occurring in response to acute stress (Kemp et al., 2022). Thus, different stimuli may trigger TNF production from the different types of glia. This work, though, makes a clear case for astrocytes being the cell type monitoring the overall network activity to trigger HSP.

It is interesting to note that though deletion of TNF from microglia did not result in an abrogation of synaptic scaling, it did result in a decrease in baseline mEPSC amplitude (Fig. 3B,C). Similarly, microglia have been shown to be required
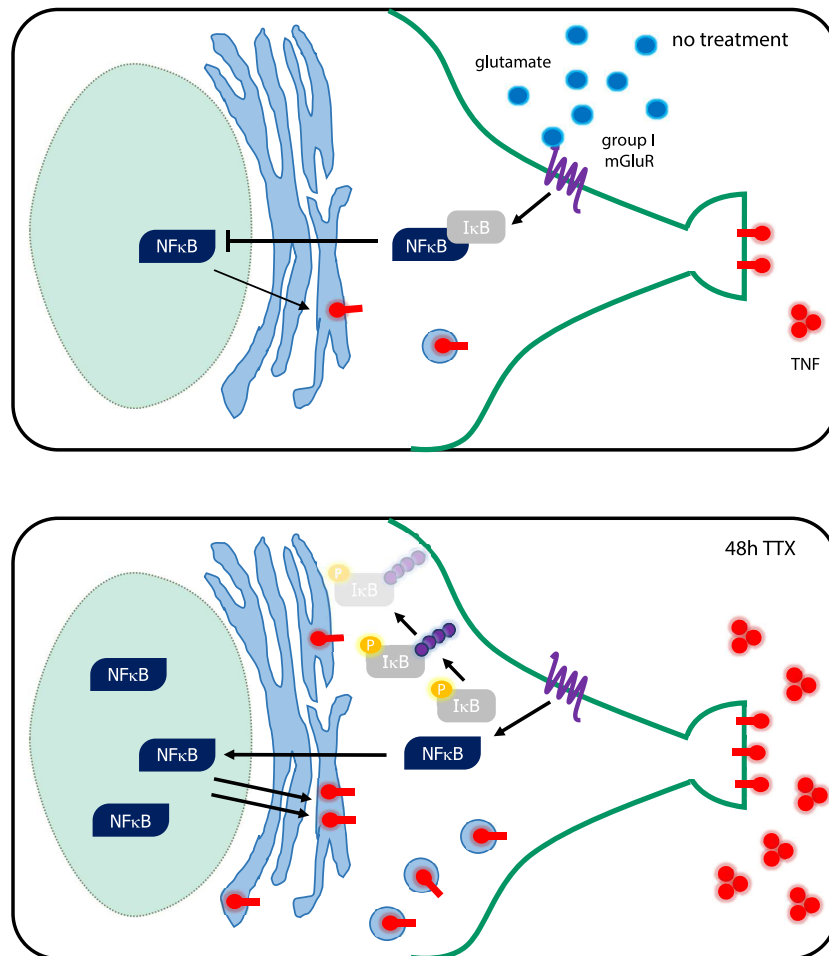
Figure 6. Summary of TNF regulation by glutamate in astrocytes during synaptic scaling. (No treatment) under normal conditions, glutamate from synapses activates type I mGluRs on astrocytes, which leads to the sequestration of NFκB in the cytoplasm by high levels of IκB. This results in a low level of TNF expression. (48 h TTX) During activity deprivation, glutamate levels coming from synapses decreases, resulting in less activation of type I mGluRs. This leads to a decrease in IκB levels through its ubiquitination and proteasomal degradation, relieving the suppression of NFκB activity, resulting in increased TNF production.

for the maintenance of synaptic structure in the visual system (Wang et al., 2016), although the TNF dependence of this effect was not assessed. It should be noted that there is a slight background difference between the GFAP-Cre and CS3CR1-Cre animals, although the lines were back-crossed for five or more generations. More work will be necessary to understand the impact of microglial TNF on the regulation of basal synaptic function.

Taken together, the data presented here describe a potential signaling pathway underlying the astrocytic secretion of TNF during synaptic scaling (Fig. 6). Under baseline conditions, glutamate released from synapses activates group I mGluRs on astrocytes. Downstream of the G_q signaling, NFκB activation is blocked through the stabilization of IκB and subsequent sequestration of NFκB in the cytoplasm, which in turn, decreases TNF production. When cultures are treated with 48 h TTX, reduced extracellular glutamate no longer activates mGluRs, and this results in decreased IκB levels due to its phosphorylation, ubiquitination, and degradation by the proteasome. This allows NFκB to move to the nucleus and drive transcription of the TNF gene. While we can exclude a role of NFκB in the neuronal response to TNF, the current data do not have the precision to exclude a role for NFκB in the release of some neuronal factor to signal to the astrocyte. Given the known role of NFκB in

regulating TNF production, however, the proposed model is the most likely.

It is interesting to note that group I mGluRs have previously been linked to synaptic scaling, although that report indicates that they are engaged in neurons in response to activity elevation in order to mediate downscaling of synaptic strength (Hu et al., 2010). While the mechanism is certainly distinct from what we describe here, it does indicate that group I mGluRs can be players in the homeostatic regulation of synaptic strength. It is also intriguing that the net result of group I mGluR activation is the same in both cases: a decrease in synaptic strength.

The signaling pathway outlined here is plausible for astrocytes during development, when the group I mGluR mGluR5 expression is relatively high (Sun et al., 2013). The cultured preparations used here likely reflect somewhat early developmental timepoints. However, mGluR5 expression is substantially lower in adult astrocytes (Sun et al., 2013; Sardar et al., 2021), although some DHPG response remains. Whether this signaling pathway remains relevant in adult tissue or homeostatic signaling of activity levels shifts to other pathways will require further investigation. It is interesting to note that the homeostatic component of ocular dominance plasticity in the visual cortex is TNF dependent during the critical period (Kaneko et al., 2008) but TNF independent in the adult (Ranson et al., 2012). On the other

hand, astrocytic TNF production is important for the behavioral response to antidepressants in adult mice (Duseja et al., 2014).

The present study provides important information on the mechanism of synaptic scaling, with clear identification of the cellular players involved. In addition to providing insight into the basic functioning of neural circuits and their maintenance, deeper understanding of the pathways may also allow for the understanding of how these mechanisms are dysregulated in pathological conditions. Considering TNF production is a hallmark of many disease and injury states, the importance of understanding the biological processes that may be disrupted in these situations becomes even more apparent.

References

Bajenaru ML, Zhu Y, Hedrick NM, Donahoe J, Parada LF, Gutmann DH (2002) Astrocyte-specific inactivation of the neurofibromatosis 1 gene (NF1) is insufficient for astrocytoma formation. Mol Cell Biol 22:5100–5113.

Beattie EC, Stellwagen D, Morishita W, Bresnahan JC, Ha BK, Von Zastrow M, Beattie MS, Malenka RC (2002) Control of synaptic strength by glial TNF alpha. Science 295:2282–2285.

Becker D, Zahn N, Deller T, Vlachos A (2013) Tumor necrosis factor alpha maintains denervation-induced homeostatic synaptic plasticity of mouse dentate granule cells. Front Cell Neurosci 7:257.

Ben Achour S, Pascual O (2010) Glia: the many ways to modulate synaptic plasticity. Neurochem Int 57:440–445.

Brewer GJ, Torricelli JR, Evege EK, Price PJ (1993) Optimized survival of hippocampal neurons in B27-supplemented neurobasal, a new serum-free medium combination. J Neurosci Res 35:567–576.

Carballo E, Lai WS, Blackshear PJ (1998) Feedback inhibition of macrophage tumor necrosis factor-alpha production by tristetraprolin. Science 281: 1001–1005.

Chen L, Li X, Tjia M, Thapliyal S (2022) Homeostatic plasticity and excitation-inhibition balance: the good, the bad, and the ugly. Curr Opin Neurobiol 75:102553.

Chung IY, Benveniste EN (1990) Tumor necrosis factor-alpha production by astrocytes. Induction by lipopolysaccharide, IFN-gamma, and IL-1 beta. J Immunol 144:2999–3007.

Chung WS, Barres BA (2012) The role of glial cells in synapse elimination. Curr Opin Neurobiol 22:438–445.

Cornell-Bell AH, Finkbeiner SM, Cooper MS, Smith SJ (1990) Glutamate induces calcium waves in cultured astrocytes: long-range glial signaling. Science 247:470–473.

Dailey ME, Waite M (1999) Confocal imaging of microglial cell dynamics in hippocampal slice cultures. Methods 18:222–230; 177.

Dani JW, Chernjavsky A, Smith SJ (1992) Neuronal activity triggers calcium waves in hippocampal astrocyte networks. Neuron 8:429–440.

Dong Y, Benveniste EN (2001) Immune function of astrocytes. Glia 36:180–190.

Duseja R, Heir R, Lewitus GM, Altimimi HF, Stellwagen D (2014) Astrocytic TNF alpha regulates the behavioral response to antidepressants. Brain Behav Immun 44:187–194.

Eroglu C, Barres BA (2010) Regulation of synaptic connectivity by glia. Nature 468:223–231.

Falvo JV, Tsytsykova AV, Goldfeld AE (2010) Transcriptional control of the TNF gene. Curr Dir Autoimmun 11:27–60.

Gordon GR, Iremonger KJ, Kantevari S, Ellis-Davies GC, MacVicar BA, Bains JS (2009) Astrocyte-mediated distributed plasticity at hypothalamic glutamate synapses. Neuron 64:391–403.

Guerrini L, Blasi F, Denis-Donini S (1995) Synaptic activation of NF-kappa B by glutamate in cerebellar granule neurons in vitro. Proc Natl Acad Sci U S A 92:9077–9081.

Hailer NP, Jarhult JD, Nitsch R (1996) Resting microglial cells in vitro: analysis of morphology and adhesion molecule expression in organotypic hippocampal slice cultures. Glia 18:319–331.

Hanisch UK (2002) Microglia as a source and target of cytokines. Glia 40:140–155.

Hayden MS, West AP, Ghosh S (2006) NF-kappaB and the immune response. Oncogene 25:6758–6780.

Heir R, Stellwagen D (2020) TNF-mediated homeostatic synaptic plasticity: from in vitro to in vivo models. Front Cell Neurosci 14:565841.

Henneberger C, Papouin T, Oliet SH, Rusakov DA (2010) Long-term potentiation depends on release of D-serine from astrocytes. Nature 463:232–236.

Hogan-Cann AD, Anderson CM (2016) Physiological roles of non-neuronal NMDA receptors. Trends Pharmacol Sci 37:750–767.

Hu JH, et al. (2010) Homeostatic scaling requires group I mGluR activation mediated by Homer1a. Neuron 68:1128–1142.

Jones EV, Bernardinelli Y, Tse YC, Chierzi S, Wong TP, Murai KK (2011) Astrocytes control glutamate receptor levels at developing synapses through SPARC-beta-integrin interactions. J Neurosci 31:4154–4165.

Kaltschmidt C, Kaltschmidt B, Baeuerle PA (1995) Stimulation of ionotropic glutamate receptors activates transcription factor NF-kappa B in primary neurons. Proc Natl Acad Sci U S A 92:9618–9622.

Kaneko M, Stellwagen D, Malenka RC, Stryker MP (2008) Tumor necrosis factor-alpha mediates one component of competitive, experience-dependent plasticity in developing visual cortex. Neuron 58:673–680.

Kemp GM, Altimimi HF, Nho Y, Heir R, Klyczek A, Stellwagen D (2022) Sustained TNF signaling is required for the synaptic and anxiety-like behavioral response to acute stress. Mol Psychiatry 27:4474–4484.

Kontoyiannis D, Pasparakis M, Pizarro TT, Cominelli F, Kollias G (1999) Impaired on/off regulation of TNF biosynthesis in mice lacking TNF AU-rich elements: implications for joint and gut-associated immunopathologies. Immunity 10:387–398.

Kuprash DV, et al. (2005) Novel tumor necrosis factor-knockout mice that lack Peyer's patches. Eur J Immunol 35:1592–1600.

Lewitus GM, Konefal SC, Greenhalgh AD, Pribiag H, Augereau K, Stellwagen D (2016) Microglial TNF-alpha suppresses cocaine-induced plasticity and behavioral sensitization. Neuron 90:483–491.

McCarthy KD, de Vellis J (1980) Preparation of separate astroglial and oligodendroglial cell cultures from rat cerebral tissue. J Cell Biol 85:890–902.

Methot L, Hermann R, Tang Y, Lo R, Al-Jehani H, Jhas S, Svoboda D, Slack RS, Barker PA, Stifani S (2013) Interaction and antagonistic roles of NF-kappaB and Hes6 in the regulation of cortical neurogenesis. Mol Cell Biol 33:2797–2808.

Niswender CM, Conn PJ (2010) Metabotropic glutamate receptors: physiology, pharmacology, and disease. Annu Rev Pharmacol Toxicol 50:295–322.

O'Riordan KJ, et al. (2006) Regulation of nuclear factor kappaB in the hippocampus by group I metabotropic glutamate receptors. J Neurosci 26:4870–4879.

Paolicelli RC, et al. (2011) Synaptic pruning by microglia is necessary for normal brain development. Science 333:1456–1458.

Perea G, Araque A (2005) Glial calcium signaling and neuron-glia communication. Cell Calcium 38:375–382.

Perea G, Araque A (2007) Astrocytes potentiate transmitter release at single hippocampal synapses. Science 317:1083–1086.

Perea G, Navarrete M, Araque A (2009) Tripartite synapses: astrocytes process and control synaptic information. Trends Neurosci 32:421–431.

Porter JT, McCarthy KD (1996) Hippocampal astrocytes in situ respond to glutamate released from synaptic terminals. J Neurosci 16:5073–5081.

Ranson A, Cheetham CE, Fox K, Sengpiel F (2012) Homeostatic plasticity mechanisms are required for juvenile, but not adult, ocular dominance plasticity. Proc Natl Acad Sci U S A 109:1311–1316.

Sardar D, Lozzi B, Woo J, Huang TW, Cvetkovic C, Creighton CJ, Krencik R, Deneen B (2021) Mapping astrocyte transcriptional signatures in response to neuroactive compounds. Int J Mol Sci 22:3975.

Sawada M, Kondo N, Suzumura A, Marunouchi T (1989) Production of tumor necrosis factor-alpha by microglia and astrocytes in culture. Brain Res 491:394–397.

Schafer DP, Lehrman EK, Kautzman AG, Koyama R, Mardinly AR, Yamasaki R, Ransohoff RM, Greenberg ME, Barres BA, Stevens B (2012) Microglia sculpt postnatal neural circuits in an activity and complement-dependent manner. Neuron 74:691–705.

Smith JA, Das A, Ray SK, Banik NL (2012) Role of pro-inflammatory cytokines released from microglia in neurodegenerative diseases. Brain Res Bull 87:10–20.

Stellwagen D, Malenka RC (2006) Synaptic scaling mediated by glial TNF-alpha. Nature 440:1054–1059.

Stellwagen D, Beattie EC, Seo JY, Malenka RC (2005) Differential regulation of AMPA receptor and GABA receptor trafficking by tumor necrosis factor-alpha. J Neurosci 25:3219–3228.

Stence N, Waite M, Dailey ME (2001) Dynamics of microglial activation: a confocal time-lapse analysis in hippocampal slices. Glia 33:256–266.

Stoppini L, Buchs PA, Muller D (1991) A simple method for organotypic cultures of nervous tissue. J Neurosci Methods 37:173–182.

Sun W, McConnell E, Pare JF, Xu Q, Chen M, Peng W, Lovatt D, Han X, Smith Y, Nedergaard M (2013) Glutamate-dependent neuroglial calcium signaling differs between young and adult brain. Science 339:197–200.

Thiele DL, Kurosaka M, Lipsky PE (1983) Phenotype of the accessory cell necessary for mitogen-stimulated T and B cell responses in human peripheral blood: delineation by its sensitivity to the lysosomotropic agent, L-leucine methyl ester. J Immunol 131:2282–2290.

Tremblay ME, Lowery RL, Majewska AK (2010) Microglial interactions with synapses are modulated by visual experience. PLoS Biol 8: e1000527.

Turrigiano G (2007) Homeostatic signaling: the positive side of negative feedback. Curr Opin Neurobiol 17:318–324.

Uliasz TF, Hamby ME, Jackman NA, Hewett JA, Hewett SJ (2012) Generation of primary astrocyte cultures devoid of contaminating microglia. Methods Mol Biol 814:61–79.

Ullian EM, Sapperstein SK, Christopherson KS, Barres BA (2001) Control of synapse number by glia. Science 291:657–661.

Wake H, Moorhouse AJ, Jinno S, Kohsaka S, Nabekura J (2009) Resting microglia directly monitor the functional state of synapses in vivo and determine the fate of ischemic terminals. J Neurosci 29:3974–3980.

Wang X, et al. (2016) Requirement for microglia for the maintenance of synaptic function and integrity in the mature retina. J Neurosci 36:2827–2842.

Yang Y, Ge W, Chen Y, Zhang Z, Shen W, Wu C, Poo M, Duan S (2003) Contribution of astrocytes to hippocampal long-term potentiation through release of D-serine. Proc Natl Acad Sci U S A 100:15194–15199.

Yona S, et al. (2013) Fate mapping reveals origins and dynamics of monocytes and tissue macrophages under homeostasis. Immunity 38:79–91.